PHYSICAL REVIEW A, VOLUME 63, 011801(R)

Modified spontaneous emission spectra of laser dye in inverse opal photonic crystals

Henry P. Schriemer,* Henry M. van Driel,† A. Femius Koenderink, and Willem L. Vos‡
Van der Waals–Zeeman Instituut, Universiteit van Amsterdam, 1018 XE Amsterdam, The Netherlands§
(Received 10 August 2000; published 13 December 2000)

We have observed strongly modified spontaneous-emission spectra from laser dye in photonic crystals made of inverse opals in titania (TiO_2). We identify stop bands with large relative widths of 15%, comparable to the dyes' emission spectrum, and 75% attenuation of the emission strength. For a wide range of angles, two stop bands are simultaneously manifested; their angle-dependent frequencies display an avoided crossing that is corroborated by reflectivity experiments. The edges of the stop bands agree well with band-structure calculations, but differ from simple Bragg diffraction as a result of multiple wave coupling. The strongly reduced dispersion of the Bloch modes likely causes a significant change in the density of states.

DOI: 10.1103/PhysRevA.63.011801 PACS number(s): 42.50.Ct, 42.70.Qs, 42.25.Fx, 81.05.Zx

Photonic crystals are receiving intense scrutiny, not only as regards the novel physics they embody [1,2], but also as the underlying architecture for all-optical microchips [3]. Widely pursued to control the atom's spontaneous-emission rate [1,4], photonic crystals are periodic dielectric composites that control light propagation by Bragg diffraction [7], since the periodicity of the refractive-index variations is on the order of the wavelength of light [5,6]. The achievement of a full photonic band gap, a range of frequencies for which the Bragg diffractions simultaneously inhibit light propagation for all directions and polarizations, is the *raison d'être* for three-dimensional photonic crystals. Photonic band-gap crystals will not only influence emission spectra but, as the density of states vanishes inside such gaps, also emission rates; intricate dynamics are expected [8]. Even in the absence of photonic band gaps, important advances in the control of emission have already been made in two-dimensional structures, producing, for example, efficient miniature lasers [9].

Previous studies of embedded dyes [10,11] and semiconductors [12] in three-dimensional weakly photonic crystals have revealed modified emission spectra. The luminescence was inhibited in particular directions, forming stop gaps whose frequencies depend on angle, in accordance with Bragg diffraction by a single set of lattice planes. No significantly altered emission lifetimes have been observed, however, because the densities of states are hardly modified [13,14]. The observed minor changes in lifetime agree well with the few percent reduction in total solid angle for light propagation due to Bragg diffraction [11], as a result of the low dielectric contrasts involved and the crystals' weak interaction with light.

Recently, novel photonic crystals have been developed from materials with high dielectric constants [15,16]. These so-called air-sphere crystals, or inverse opals, interact so strongly with light that the propagation of light is inhibited for more than 55% of all directions [17]. Here, we investigate spontaneous emission of laser dye inside such crystals and identify a mechanism by which the directional properties of the spectrum are modified. For emission in directions nearly normal to the (111) lattice planes, we observe single Bragg stop bands. For emission directions between 25° and 55°, however, *dual* stop bands are observed in the emission spectra, with unprecedented large widths of 15%. The angular dependence of the central frequencies of these stop bands display an avoided crossing, characteristic of coupled modes. This behavior agrees with complementary reflectivity results [18] and with theoretically calculated dispersion curves. It appears that the emission spectra are strongly modified by simultaneous diffraction from (111) and (200) crystal planes. The avoided crossing is a manifestation of three-dimensional confinement, since the first Brillouin zone of an fcc crystal is fully enclosed by the (111) and (200) Bragg planes and their symmetry-related equivalents. Multiple diffraction results in Bloch modes with little dispersion, which is the basis for the formation of photonic band gaps. Such modes likely cause significant changes in the density of states, thus paving the way to novel quantum optical effects [8].

The photonic crystals studied here are fcc crystals of air spheres in titania (see Fig. 1), with lattice parameters varying between $a = 480$ and 510 nm, and a dielectric contrast ranging from 6.25 to 6.5; for a detailed description and characterization, see Ref. [16]. The samples have overall dimensions on the order of millimeters and are composed of a number of high-quality crystal domains with diameters as large as 50 μm. To incorporate the dye, the air-sphere crystals were immersed in a dilute solution of Nile Blue [19] in ethanol (~ 70 μmol/l) for 24 h to promote the adsorption of dye molecules at the TiO_2-air interfaces of the voids (see Fig. 1), and then rinsed and dried. To ensure emission from solely internal sources, the dye adsorbed near the external sample surface was first selectively bleached by illuminating the photonic crystal with an intense laser beam (wavelength $\lambda = 514$ nm) at the Bragg angle; see Ref. [11].

The optical setup used to measure emission spectra is shown in Fig. 1. The dye inside the crystals was excited with a *p*-polarized laser beam incident at angles away from the Bragg angle (for $\lambda = 514$ nm), and focused to ~ 30 μm in

*Present address: Zenastra Photonics Inc., Ottawa, Canada K1G 4J8; email address: henry.schriemer @zenastra.com
†Permanent address: Department of Physics, University of Toronto, Toronto, Canada M5S 1A7.
‡Email address: wvos@wins.uva.nl
§URL: www.thephotonicbandgaps.com

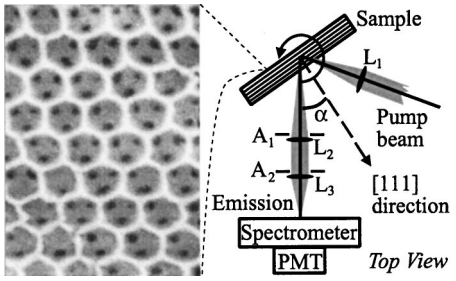

FIG. 1. Right: scheme of the optical setup. A pump beam ($\lambda = 514$ nm), focused by lens L_1 excites the dye inside the photonic crystal. Emitted light is collected at an angle α to the normal of the sample [i.e., normal to the (111) lattice planes] by lenses L_2, L_3, and apertures A_1, A_2, dispersed by a grating spectrometer, and detected with a photomultiplier tube (PMT). Left: scanning electron micrograph of a typical surface of an inverse opal in TiO_2, showing the hexagonal arrangement (111 plane) of air spheres ($a = 501 \pm 7$ nm). Dark circles are windows that connect the air spheres to the next lattice plane [16].

diameter. The sample was mounted in a goniometer to acquire emission as a function of detection angle α from the normal to the (111) planes. For $\alpha = 0°$, the (111) planes are normal to the detection axis of the spectrometer. The alignment of the laser beam on the sample was monitored through a microscope. Due to spectrometer grating efficiencies, principally the *p*-polarized component was detected by the photomultiplier tube. Emission spectra were acquired in 5° steps, with an angular resolution of 5°. Due to the very low concentration of adsorbed dye (estimated at $\sim 10^2$ molecules per air sphere), and concomitant low fluorescence, several spectra were averaged and smoothed, yielding an effective spectral resolution of ~ 100 cm^{-1}. Detector dark count and stray light background have been subtracted. The measured intensities of all spectra recorded at the various angles have been adjusted to overlay their low- or high-frequency ranges, where no crystal effects are observed, to correct for the angle-dependent variation in detection efficiency [11]. Techniques for measuring reflectivity are described in Refs. [17,18,20].

The emission spectra at select detection angles for a crystal with $a = 501$ nm are presented in Fig. 2(A). For emission directions in excess of 60° [Fig. 2(A) magenta curve], appreciable modification of the spectral line shape ceased, and the high-frequency edge of the emission spectrum has the same characteristic spectral shape as seen at low detection angles, between 0° and 25°. This implies that the $\alpha = 60°$ stop band of the crystal does not overlap the emission spectrum of the dye. In comparison, at $\alpha = 0°$ [Fig. 2(A) red curve], the photonic crystal greatly suppresses emission over a wide spectral range, from 14 000 to 16 500 cm^{-1}. With increasing emission angle, the low-frequency components of the emission spectra recover, and the frequency range of suppressed emission moves toward high frequencies, as expected for photonic crystal stop bands due to a single Bragg diffraction. It was demonstrated that the line shape was independent of the pump intensity, and that the emitted intensity was linear with the pump power; hence lasing or amplified spontaneous emission effects can be excluded. By discretely traversing

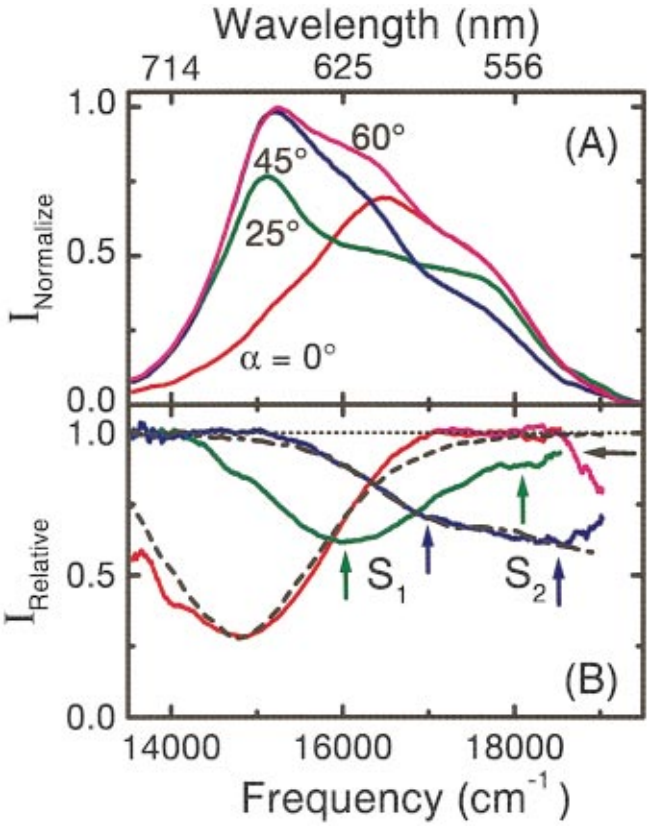

FIG. 2. (Color) (A) Normalized emission spectra as a function of frequency in wave numbers for Nile Blue in a titania inverse opal ($a = 501$ nm). (B) Relative intensities, obtained from the spectra in (A). Red curves are obtained at an angle $\alpha = 0°$, green curves at $\alpha = 25°$, blue curves at $\alpha = 45°$, and magenta curves at $\alpha = 60°$. Colored arrows are center frequencies of S_1 and S_2 stop bands. Reflectivity data in (B) are shown for $\alpha = 0°$ and 45° (dashed and dashed-dotted curve).

sample faces with the focused pump beam, the spectral line shapes were found to be well reproduced on the same sample for all angles. Experiments on crystals with a lattice parameter of 480 nm revealed emission spectra with stop bands centered at 15 500 cm^{-1} at $\alpha = 0°$ and band frequencies increasing with angle, which confirms that the observed features are indeed a photonic crystal effect. It is readily apparent that the relative width of the stop band is very broad ($\Delta\omega/\omega = 15\%$), so broad that it is comparable to the broad spectral range of the dye; the large width is a signature of a photonic crystal that strongly interacts with light.

We extract the stop bands, i.e., the directional emission properties, by exploiting data from one and the same sample, thus avoiding uncertainties in comparing samples. If there is negligible stop-band overlap, dividing the emission at α_1 by the emission at α_2 gives the stop band at α_1 for values less than unity, and the stop band at α_2 is found from the inverse ratio. For example, since the blue edges of the emission spectra are the same at $\alpha_1 = 0°$ and $\alpha_2 = 60°$, their stop bands will clearly not overlap [Fig. 2(A), red and magenta curves, respectively], as is indeed demonstrated by the ratios, shown in Fig. 2(B) (red and magenta curves, respectively), that quantify these stop bands. For overlapping stop bands,

the low- and high-frequency edges are extracted separately by dividing α_1 spectra by α_2 spectra ($\alpha_1 < \alpha_2$) until the edge ratios converge. The low-frequency edge of the α_1 stop band is obtained by dividing the α_1 spectrum by emission spectra for increasing α_2; the line shape of the ratio will converge as the difference between α_1 and α_2 increases. Similarly, the high-frequency edge at α_2 is obtained by noting the convergence of the inverse ratio as α_1 is decreased. While we noted weakly sample-dependent emission line shapes (due to differences in doping conditions), the line-shape ratios are sample independent, hence the stop bands are unambiguously determined. Figure 2(B) clearly demonstrates that the photonic periodicity imposes a strong attenuation on the transfer of radiant energy to free space.

Naively, one would expect the emission to completely vanish at the center of a stop band. We observe, however, an attenuation up to 75% near the center of the gap at $\alpha = 0°$. Limited attenuation has been seen previously [10–12], and was attributed to diffuse scattering by intrinsic defects near the external crystal-air interface [11]. The pertinent mechanism in the present case is related: since the mean-free path $l \sim 15$ μm [21] is much smaller than the ~ 200 μm sample thickness, light propagates diffusively in the bulk of the samples. Diffuse light emanating from a depth $z < l$ from the crystal-air interface propagates ballistically to the interface, but may be redirected to the detector by scattering from intrinsic defects. Since l is larger than the attenuation length for Bragg diffraction l_B (typically $l_B \sim l \times 0.2$ to 0.5 [21]), light scattered at $z < l_B$ is hardly Bragg attenuated, while light scattered at $l_B < z < l$ reveals a stop band. This simple model predicts a total attenuation in the stop band of about 50% to 80%, in agreement with our observations.

At low emission angles [e.g., at $\alpha = 0°$, Fig. 2(B), red curve], single broad stop bands are revealed. Interestingly, at higher angles there appears to be a transition to a *double* stop band: the first clear evidence of this is for $\alpha = 25°$ at $\sim 18\,000$ cm^{-1} [Fig. 2(B), green arrows]. We denote the lower-frequency stop bands by S_1, and the higher-frequency stop bands by S_2. With increasing angle, this second stop band becomes more apparent while S_1 decreases in amplitude. The intensity ratio for $\alpha = 45°$ [Fig. 2(B), blue arrows] shows evidence of an S_1 feature at 17 000 cm^{-1} and a strong S_2 feature at 18 700 cm^{-1}. By $\alpha = 60°$, the S_1 band has vanished and the low-frequency edge of S_2 has moved beyond 18 500 cm^{-1} (black arrow), leaving the spectrum essentially unsuppressed. It is clear that the observed phenomena cannot be explained by simple Bragg diffraction [7], but are likely a coupled wave phenomenon.

To further investigate whether the light emitted by internal sources indeed probes the photonic band structure, we have performed reflectivity experiments on the same sample using externally incident plane waves, since this technique readily identifies the central frequencies and widths of stop bands [17,18]. To facilitate direct comparison, we represent the reflectivity data R as $1 - \beta R$, where β is a scaling constant accounting for differences in probe geometries and physical properties. The maximum reflectivity at normal incidence was limited to 20%, due to the use of a large probe beam (500 μm) that samples grain boundaries between multiple domains [17]. We show representative reflectivity results in Fig. 2(B): for $\alpha = 0°$ (dashed curve) a single stop band is revealed, and for $\alpha = 45°$ (dash-dotted curve) a double stop band is again found, in agreement with the emission data. There are minor differences between the reflectivity and emission data; e.g., in the angular range where the avoided crossing sets in or the bandwidth over which the crossing takes place. On the whole, there is good agreement between the single and double stop bands in emission and in reflectivity, confirming that the avoided crossings observed in the strongly modified emission spectra are indeed caused by photonic gaps.

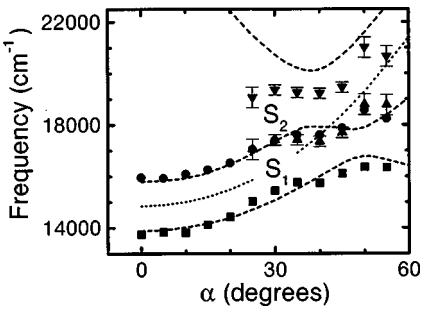

FIG. 3. Angular dependence of the stop band edges, determined from spectra as in Fig. 2(B). The squares and circles are the lower and upper edges, respectively, of the S_1 stop band; the triangles and inverted triangles are the lower and upper edges, respectively, of the S_2 stop band. The dashed curves are frequencies calculated from the photonic band structures using the plane-wave expansion method, and the dotted curve is the center frequency assuming single (111) Bragg diffraction.

Figure 3 shows the frequencies of the stop bands as a function of α by delineating upper and lower edges by their full widths at half maxima (FWHM, solid symbols). In the absence of crystal imperfections such as strain, the FWHM of reflectivity or emission stop bands are heuristic but reliable measures of the widths of stop gaps in dispersion relations [11,17]. The central frequencies (not shown) and widths were obtained by fitting Gaussian functions to the data in Fig. 2(B); the widths of the double gaps at higher emission angles are unambiguously determined from a two-Gaussian fit. For comparison, we have also plotted in Fig. 3 the angular dependence of the central frequency for Bragg diffraction by a single set of (111) planes (dotted curve). We find that, for emission angles up to 30°, the center of the measured S_1 stop band agrees very well with the simple Bragg behavior. Near $\alpha = 30°$, there is a marked departure from simple Bragg diffraction, with a depression of S_1 to lower frequencies and the appearance of a higher-frequency stop band S_2.

Since the emission stop bands agree well with reflectivity results, we have performed plane-wave band-structure calculations (see Refs. [5,6]) to investigate the angle-dependent features. The crystal is described by a position-dependent dielectric function $\varepsilon(\mathbf{r})$ based on experimental observations of the structure of the crystals [16,18,20]. The model consists of overlapping shells of dielectric material (TiO_2), with inner radius $R = a/(2\sqrt{2})$, outer radius $1.09R$, and cylindrical windows of radius $0.4R$ connecting neighboring air spheres (cf. Fig. 1). The frequencies of the Bloch modes are calcu-

lated as a function of wave vector, with the latter converted to angle using momentum conservation parallel to the sample surface; the dashed curves in Fig. 3 show the results. The two curves that start at $\alpha = 0°$ are the mixed (000) and (111) modes that bound the (111) Bragg diffraction stop gap. It is clear that the calculated modes agree very well with the edges of the emission stop band S_1. The intermediate and highest frequency modes agree well with the edges of the S_2 stop band. The observed avoided crossing behavior is due to the (200) Bloch mode (which decreases in frequency) that mixes with the (000) and (111) modes. This has also recently been observed in reflectivity [18]. It is clear that in the range of the avoided crossing, the intermediate mode is repelled by the outer two ones and becomes nearly dispersionless. This is expected to lead to a modification of the density of states in this particular frequency range.

A photonic band gap in strongly interacting photonic crystals can be regarded as fully dispersionless modes for all directions simultaneously (i.e., all angles in Fig. 3). Recently, complex reflectivity features have been observed in the frequency range where fcc crystals will develop a photonic band gap [20,22], which has been interpreted as a complex multiple Bragg diffraction phenomenon [20]. The identification of relevant spectral features by us is thus an important step towards the understanding of emission spectra in the frequency range of a photonic band gap.

We thank Judith Wijnhoven for preparing the crystals, Mischa Megens and Rudolf Sprik for discussions, and Ad Lagendijk for continuous support. This work is part of the research program of the ''Stichting voor Fundamenteel Onderzoek der Materie (FOM),'' which is supported by the ''Nederlanse Organisatie voor Wetenschappelijk Onderzoek'' (NWO). H.M.v.D. thanks Ad Lagendijk for making his stay possible with support from NWO.

[1] E. Yablonovitch, Phys. Rev. Lett. **58**, 2059 (1987).
[2] S. John, Phys. Rev. Lett. **58**, 2486 (1987).
[3] A. Chutinan and S. Noda, Appl. Phys. Lett. **75**, 3739 (1999).
[4] M. O. Scully and M. S. Zubairy, *Quantum Optics* (Cambridge University Press, Cambridge, 1997).
[5] J. D. Joannopoulos, R. D. Meade, and J. N. Winn, *Photonic Crystals* (Princeton University Press, Princeton, NJ, 1995).
[6] *Photonic Band Gap Materials*, edited by C. M. Soukoulis (Kluwer, Dordrecht, 1996).
[7] R. W. James, *The Optical Principles of the Diffraction of X-Rays* (Bell, London, 1954).
[8] N. Vats and S. John, Phys. Rev. A **58**, 4168 (1998); E. Paspalakis, N. J. Kylstra, and P. L. Knight, *ibid.* **60**, R33 (1999); G. M. Nikolopoulos and P. Lambropoulos, *ibid.* **61**, 053812 (2000); Y. Yang and S. Y. Zhu, *ibid.* **62**, 013805 (2000); Z. Y. Li, L. L. Lin, and Z. Q. Zhang, Phys. Rev. Lett. **84**, 4341 (2000).
[9] O. Painter *et al.*, Science **284**, 1819 (1999); C. J. M. Smith *et al.*, Electron. Lett. **35**, 228 (1999).
[10] V. N. Bogomolov *et al.*, Phys. Rev. E **55**, 7619 (1997); T. Yamasaki and T. Tsutsui, Appl. Phys. Lett. **72**, 1957 (1998); Y. Yoshino *et al.*, *ibid.* **73**, 3506 (1998).
[11] M. Megens, J. E. G. J. Wijnhoven, A. Lagendijk, and W. L. Vos, J. Opt. Soc. Am. B **16**, 1403 (1999).
[12] S. G. Romanov *et al.*, Phys. Status Solidi A **164**, 169 (1997); S. V. Gaponenko *et al.*, JETP Lett. **68**, 142 (1998); A. Blanco *et al.*, Appl. Phys. Lett. **73**, 1781 (1998).
[13] E. P. Petrov, V. N. Bogomolov, I. I. Kalosha, and S. V. Gaponenko, Phys. Rev. Lett. **81**, 77 (1999); M. Megens, H. P. Schriemer, A. Lagendijk, and W. L. Vos, *ibid.* **83**, 5401 (1999).
[14] M. Megens, J. E. G. J. Wijnhoven, A. Lagendijk, and W. L. Vos, Phys. Rev. A **59**, 4727 (1999).
[15] O. D. Velev and E. W. Kaler, Adv. Mater. **12**, 531 (2000); Y. Xia, B. Gates, Y. Yin, and Y. Lu, *ibid.* **12**, 693 (2000), and references therein.
[16] J. E. G. J. Wijnhoven and W. L. Vos, Science **281**, 802 (1998); unpublished.
[17] M. S. Thijssen *et al.*, Phys. Rev. Lett. **83**, 2730 (1999).
[18] H. M. van Driel and W. L. Vos, Phys. Rev. B **62**, 9872 (2000).
[19] U. Brackmann, *Laser Dyes* (Lambda Physik, Göttingen, 1997).
[20] W. L. Vos and H. M. van Driel, Phys. Lett. A **272**, 101 (2000).
[21] A. F. Koenderink *et al.*, Phys. Lett. A **268**, 104 (2000).
[22] A. Blanco *et al.*, Nature (London) **405**, 437 (2000).